MICHIGAN STATE UNIVERSITY

National Superconducting Cyclotron Laboratory

RARE ISOTOPE PRODUCTION NEAR THE NEUTRON DRIP LINE

W.A. FRIEDMAN, M.B. TSANG, D. BAZIN, W.G. LYNCH

MSUCL-1167

JULY 2000

Rare Isotope Production Near the Neutron Drip Line

W.A. Friedman[1], M.B. Tsang[2], D. Bazin[2], W.G. Lynch[2]
[1] Department of Physics, University of Wisconsin, Madison, WI 53706
[2] National Superconducting Cyclotron Laboratory, Michigan State University, E. Lansing, MI 48824

Abstract

The underlying mechanism involved in the production of very neutron rich isotopes using projectile fragmentation is studied with an abrasion-ablation (A-A) model. The A-A model suggests that very neutron rich isotopes are produced by removing nearly all the required protons in the non-equilibrium abrasion stage, with minimal evaporation of neutrons in the ablation stage - "cold fragmentation". Furthermore, the production of the most neutron rich nuclei from a fixed projectile relies heavily on the neutron fluctuations in the ablation stage. The production of the isotopes closest to the neutron drip line using neutron rich unstable beams is examined.

In the nuclear chart of neutron numbers versus proton numbers, all the stable isotopes, about 300 of them, are found in the so-called "valley of stability". The terra incognita of rare isotopes lying away from this valley mainly consist of three regions: a. nuclei near the neutron drip lines [1,2], b. nuclei near the proton drip lines [1,2], and c. superheavy nuclei with atomic number greater than 116 [3]. Production of these nuclei will be of great interest for the current radioactive beam facilities in the world as well as future generation of accelerators, including the Rare Isotope Accelerators (RIA), the construction of which is being studied in USA [2,4].

Even though great strides have been made in the past decade to push toward the proton and neutron drip lines, full knowledge of these isotopes with extreme proton and neutron numbers are limited to light elements up to oxygen [5]. As the proton drip lines lie closer to the valley of stability due to the Coulomb force, most of the nuclei in the proximity of the proton drip line will be explored in the coming decade. On the other hand, the neutron drip lines prove to be much more challenging experimentally, as they lie about three times further away from stable isotopes than the proton drip lines. However knowledge about these nuclei is of utmost importance to the full understanding of many processes in nuclear astrophysics and basic nuclear properties. For example, nuclei found in this region provide important pathways for nucleosynthesis [6], especially those related to the rapid neutron capture (r) process. Extremely neutron rich isotopes also provide structure information as to whether nuclear shells vanish in the "sea" of neutrons [7]. In addition, they offer opportunities to extrapolate our knowledge from these rare isotopes to properties of the bulk neutron-rich nuclear matter such as the neutron stars [8].

While theoretical calculations can provide indications of conditions for the drip lines [9], there is no substitute for direct measurements. By necessity, observations in the neutron-rich regime require the production of short-lived isotopes and beams. In the past, one of the most effective techniques has been to use projectile fragmentation as a mechanism to create such isotopes [10]. This technique continues to offer promise for the future.

The general goal of this article is to better understand the process of producing neutron-rich isotopes using projectile fragmentation. Specifically, we want to explore the most effective means to produce these isotopes. It is hoped that this study will suggest future experimental techniques toward this end.

Recent systematic studies of the effects of the isospin of reacting nuclei has identified a measurable quantity which is useful in such explorations [11, 12]. This quantity, $R_{21}(N,Z) = Y_2(N,Z)/Y_1(N,Z)$, gives the relative yields, $Y_i(N,Z)$, of all the isotopes from two reactions, 1 and 2, which differ primarily in the isospin of the reacting systems. In cases covering a wide range of energies, it is found that $R_{21}(N,Z)$ follow a very striking behavior as a function of the charge number (Z) and neutron number (N) of the isotopes. Namely, for reactions where a high degree of equilibrium is achieved, the dependence is strongly exponential in both variables, Z and N. If we follow the convention that the initial system of reaction 2 is more neutron-rich than that of reaction 1, $R_{21}(N,Z)$ gives an quantitative measure of the enhanced production of neutron-rich isotopes.

In this article, we have chosen to study the fragmentation of Kr beams because the range of neutron numbers spanned by the two stable Kr beams, ^{78}Kr and ^{86}Kr is large. While there are very few experiments that measure a large range of isotopes, such data exist for the fragmentation of both Kr isotopes [13, 14]. Figure 1 shows the observable $R_{21}(N,Z) = Y_{^{86}Kr}(N,Z)/Y_{^{78}Kr}(N,Z)$ constructed from the respective isotope yields for elements $Z = 23 - 36$, measured from the projectile fragmentation of ^{78}Kr and ^{86}Kr, as a function of N. To provide a clearer representation of the data, all even-Z isotopes are shown as solid points while the odd-Z isotopes are shown as the open points. The corresponding solid and dashed lines in the left panels are drawn to guide the eyes. It is clear that as one goes toward very neutron-rich isotopes there is a substantial rise in the value of R_{21}. For isotopes of elements, Z=28-31, there is an order of magnitude increase in isotope yield for each extra neutron. In the data for $Z < 25$, the measured R_{21} exhibits a V-shape suggesting that production of the lighter proton-rich isotopes, for example, Z=23, N=25 particles, from the neutron rich projectile is also enhanced. This observation is counter-intuitive and may arise from features other than the N/Z of the projectiles.

Because of the importance of estimating the yields of species from fragmentation of primary beams, there has been a concerted effort to phenomenologically fit the systematics of isotope yield with parameters obtained from existing fragmentation data. The program EPAX has been successfully used to develop radioactive beams [15]. (In this article, all EPAX calculations were performed with the new improved version of EPAX2.) Predicted values of R_{21} from EPAX are shown as solid and dashed lines in the right hand panel of Figure 1. The slopes of the EPAX lines in Figure 1 for the different elements are much flatter than the experimental data. There are also strong differences in the trends for the proton rich isotopes of the light charge elements.

Figure 2 shows the individual isotope cross-sections obtained in the fragmentation of ^{86}Kr (top panels) [13] and ^{78}Kr (bottom panel) [14]. All even-

Z isotopes are shown as solid points while the odd-Z isotopes are shown as the open points. Furthermore, each element (Z) is offset from its neighbors by a factor of 100; $10^{2(Z-22)}$ for $Z = 22 - 28$ (left hand panels) and $10^{2(Z-29)}$ for $Z = 29 - 35$ (right hand panels). A comparison of the experimental isotope yields from projectile fragmentation using ^{78}Kr beams and ^{86}Kr beams shows clearly that the production of neutron rich isotopes is greatly enhanced by the use of neutron rich projectiles. An enhancement of several orders of magnitude is found for many of these species. As will be explained later, presently it is not possible to obtain a reliable quantitative enhancement factors using the ^{78}Kr fragmentation data.

The dashed curves in Figure 2 are EPAX calculations. Since ^{86}Kr data (top panels) were used to obtained the fitting parameters, it is not surprising that the agreement with data is very good. For ^{78}Kr, the agreement between EPAX and data is not good, especially for the proton rich isotopes of $Z < 28$ (lower left panel). The disagreement is the largest for the lightest elements. This difference between data and predictions may be due to the experimental conditions using ^{78}Kr [14]. The experiment used a massive target, Ni, with lower beam energies (75A MeV). This combination may invalidate the assumption of limiting fragmentation used in the fit of the EPAX parameters.

In order to understand the physics underlying the enhancement of neutron rich isotope production, we rely on a microscopic, Abrasion-Ablation, (A-A) model. The abrasion stage assumes a non-equilibrium process wherein nucleons are rapidly removed from the projectile during an encounter with a stationary target. The remaining portion of the projectile is then left in an excited state. In the second stage, the excited system decays by a quasi-equilibrium process to reach the final products. Many models based on this general picture have been proposed [16-18].

In our A-A version, the first stage is modeled by the geometric shadow cast by the target on the projectile using expressions derived for early fireball models [19]. The material removed in the first stage is treated by assuming that the protons and neutrons are each uniformly distributed over the nucleus thus providing a probability factor for the removal of n neutrons and z protons, based on the assumption of no correlations [17,20]:

$$P = \binom{N_p}{n}\binom{Z_p}{z}/\binom{A_p}{a}$$

where $\binom{N_p}{n}$ is the combinatorial that gives the number of ways of choosing n out of N_p, etc., where N_p, Z_p, and A_p are the neutron number, proton number, and mass number of the full projectile and a is the removed mass.

The excitation energy of the system remaining following the first stage, $(N_p - n, Z_p - z)$, is modeled after the work of Schmidt and Gaimard [17], where the average excitation energy was found to equal 13.3 MeV per removed particle, and we take the width of this distribution to be Gaussian with a variance proportional to the number of removed particles. The proportionality-constant is fit to the examples in Ref. [17]. The excited system is then allowed to evaporate according to the formalism outlined by Friedman and Lynch[21]. This formalism follows the mean path of particle loss, arriving at a mean final system. In order to approximate the effect of the fluctuations in the ablation paths we use the following procedure. The width of the kinetic energy distribution for each emission is calculated to determine the variance of the excitation energy about the mean path of evaporation formalism. Using the separation energy for neutrons, we map this excitation energy variance onto the variance in the number of neutrons emitted. Since the shape of the fluctuation function is uncertain, we assume a Gaussian dependence on neutron number centered at the mean, and truncate the distribution at the integer value of the standard deviation plus one. We have ignored the charge fluctuations. This procedure for handling fluctuations suggests that the predictions for the most neutron rich isotopes should be more accurate with our model than the predictions for proton rich ones. The former processes are found to undergo ablation processes which involve only neutron emission, while the latter undergo ablation processes which are also sensitive to the charge fluctuations. Extending the Gaussian form for the neutron fluctuations beyond one standard deviation greatly raises the prediction of the proton rich isotopes and, to a lesser extent, enhances the predictions of the neutron-rich isotopes. Clearly future improvement in the treatment of ablation fluctuation is desirable. This completes the description of our model which is used to calculate the isotope yields shown in the figures.

Results obtained from this model are shown as solid lines in Figure 2. The agreement with data is very good for ^{86}Kr. The A-A model prediction is similar to that from EPAX calculations for both Kr beams. For ^{78}Kr, the disagreement with data remains. (The present calculations are also similar to results obtained from the A-A model of Schmidt. [17,18, 22]) If limiting fragmentation is not reached, as explained earlier, the assumption of a clean separation of the mass in the first stage of the process assumed in the model may not be valid.

In the A-A model, both the non-equilibrium process and the equilibrium stages, in combination, play important roles in populating the most neutron rich final isotopes from a given system. Figure 3 shows the paths of producing different Ni isotopes (solid points) from the fragmentation of ^{86}Kr which is denoted by the symbol in the upper right corner of the figure at Z=36 and N=50. The open points locate the charge and neutron number of the average excited nuclei, produced after the abrasion stage. Particles are evaporated (indicated by the dashed lines) from the intermediate nuclei during the ablation process. (Fluctuations in the neutron emission number have been ignored for this plot.) The production of the most neutron rich isotopes ($N > 39$) can be traced to the intermediate systems where the abrasion (non-equilibrium) stage removes nearly all the charge, while additional loss of neutrons to reach the final product occurs in the second stage (ablation).

If the path from the initial system to smaller final one were to involve equilibrium processes only, the average tendency would be to move toward the valley of stability. Consequently the population of the most neutron rich isotopes would rely entirely on fluctuations about the average process. This would seem much less efficient than the two-stage scenario described above, in which the proton removal is entirely non-equilibrium, and the burden for obtaining the desired end product is placed on the evaporation of the second stage. Thus, populating the most neutron rich isotopes requires the excitation of the intermediate system to be as low as possible. This allows for the minimal decrease in the neutron number, and the absence of further proton loss. This particular process to produce neutron-rich nuclei has recently been referred to as "cold fragmentation" [18].

From Figure 3, it is clear that the isotope production cross sections for the very neutron rich isotopes are influenced by several features. The most important ones include: the distribution of the excitation energy following the first stage; the probability for having a specific neutron to proton composition of the mass removed by abrasion; and the number of possible paths, involving combinations of the two stages, which reach the final product. The role of neutron fluctuations becomes particularly important for the production of isotopes which cannot be reached by the average-evaporation path. All the above considerations explain why the very neutron rich isotopes of each each element decrease in production cross-sections with the neutron number as shown in Figure 2. These factors become less restrictive with more neutron rich projectiles, resulting in the enhanced production of neutron-rich isotopes as observed in Figure 1.

In principle, major gains in the production of isotopes close to the edge of the drip line can be obtained by using very neutron rich (unstable) projectiles. To reach these it is necessary to rely on the fluctuations in the neutron yields. We illustrate this with a study of the production of $^{78}Ni(N = 50, Z = 28)$. Obviously, the conservation of neutron number makes it impossible to produce this isotope from the projectile fragmentation of Kr isotopes with mass less than 86. The EPAX calculations (dotdashed line in Figure 4) predict yields from the fragmentation of ^{86}Kr to ^{96}Kr. (All but 86 are unstable isotopes.) With ^{86}Kr, eight protons must be removed with no emission of neutrons. This is highly unlikely. Without relying on the fluctuation in the emission of neutrons, the A-A calculations suggest that the lightest Kr isotope that will give appreciable ^{78}Ni cross section is ^{96}Kr. If the number of evaporated neutrons is allowed to fluctuate with no truncation in the Gaussian distribution, our A-A model predicts the production of ^{78}Ni starting at ^{88}Kr as shown by the closed circles in Figure 4. These A-A calculations are about the same as EPAX predictions for most of the heavy projectiles, but deviate substantially when the process requires one or no neutrons to be evaporated after the first stage. However, when the A-A calculations are truncated to fluctuations of one standard deviation, as associated with in the results of Figure 2 above, the yields (open circles) are much smaller. With this procedure projectiles with mass less than 91 do not reach ^{78}Ni. While all calculations indicate a rise in production with increasing neutron richness of the projectile, there is normally a sharp drop in the anticipated available beam intensity when more neutron rich unstable beams are used. Thus, one must consider the possible gain in yields with secondary beams against the constraints of the drop in the beam intensity.

If the fragmentation of ^{100}Mo is used to produce the secondary beams of ^{87}Kr to ^{94}Kr, the drop in beam intensity is exponential, with a loss of about a factor of 3 for each neutron added to the beam. In Figure 4, the solid curve (with arbitrary normalization) indicates the folding of this intensity factor with the optimistic EPAX production cross sections (dot-dashed line) This suggests that net enhancement for the production of ^{78}Ni, may peak with the use of ^{89}Kr beams. However, the maximum gain is less than a factor of 10 going from ^{87}Kr to ^{89}Kr before the anticipated net yield drops with more neutron-rich Kr beams. In reality, this procedure is not practical. Even if we use a $2gm/cm^2$ thick ^{9}Be target, typical secondary beam intensity of ^{89}Kr is 20,000 particles per second, about six orders of magnitude smaller than the usual intensity obtained for primary beams such as ^{86}Kr. However, there might be incidences when the gains in the production of very neutron rich isotopes using unstable beams of neutron projectiles will be practical and necessary.

Since limited sets of data are used to provide the phenomenological fitting parameters in the EPAX calculations, it is interesting to examine situations where the predictions of our A-A model and the EPAX differ. Fragmentation of ^{96}Zr provides such an example. Figure 5, which has similar conventions as Figure 2, including truncated neutron fluctuations, shows the isotope cross-sections from the fragmentation of ^{96}Zr. There are substantial differences between the EPAX calculations (dashed lines) and our A-A model (solid lines) in the neutron-rich isotope yields. While the limited available data [23] seem to support the A-A model, the ranges of isotopes measured are too small to conclusively favor one of the two calculations. This example points to the need for high quality data with large isotope range. In general, the widths of the isotope distributions from ^{96}Zr are narrower in the EPAX predictions. Thus intensity calculations for the production of neutron rich beams using EPAX calculations, as is common practice, might be too conservative. The possibility of enhanced production of neutron rich beams would be a welcome relief.

In summary, we have experimentally observed the general enhanced production of neutron-rich isotopes with neutron rich beams. EPAX and A-A calculations agree well with the fragmentation data for ^{86}Kr. However, we note that neither accounts well for the ^{78}Kr data which are obtained with heavier targets and lower energy. The differences between our A-A model predictions and EPAX calculations for the fragmentation of ^{96}Zr would require more data with large mass range to resolve. If the predictions of the A-A model are correct, production of neutron-rich isotopes from the fragmentation of nuclei around this mass range could gain a factor of 10.

Using the abrasion-ablation model, we gain insight into the underlying mechanism involved in the production of the neutron rich isotopes approaching the neutron drip line. The calculations suggest that this mechanism involves the removal of all the required protons in the non-equilibrium abrasion stage, with minimal evaporation of neutrons in the ablation stage. This requires minimum excitation energy left in the intermediate stage. This picture accounts well for the variation in isotope production with the isospin of the projectile. Finally we suggest that the production of the isotopes closest to the neutron drip line may benefit from the use of neutron rich unstable beams. In that case the enhanced productions will require a balance between beam intensity and the cross section for production of the desired isotope. This may be accomplished by a systematic survey of various combinations of stable and secondary beams.

The authors wish to thank Dr. Klaus Suemmerer for providing the EPAX2 code and the digitized data for the many fragmentation data he has collected over the years. We have benefited greatly from the many discussions we have had with him and Dr. Karl Heinz Schmidt. This work is supported by the National Science Foundation under Grant Numbers

PHY-96-05140 and PHY-95-28844.

References:

[1] Scientific Opportunities with an Advanced ISOL Facility, http://www.phy.anl.gov/div/W_Pa

[2] Scientific Opportunities with Fast Fragmentation Beams from the Rare Isotope Accelerator, http://www.nscl.msu.edu/research/ria/whitepaper.pdf

[3] V. Ninov et al., Phys. Rev. Lett. **83**, 1104 (1999).

[4] Report of the Isotope Separation On-Line (ISOL) task force to the Nuclear Science Advisory Committee (NSAC) http://srfsrv.jlab.org/isol/ISOLTaskForceReport.pdf

[5] D. Guillemaud-Mueller et al., Phys. Rev. **C 41**, 937 (1990).

[6] H. Schatz et al., Phys. Rep.**294**, 168 (1998).

[7] J. Dobaczewski, W. Nazarewicz, and T. Werner, Phys. Rev. **C 53**, 2809 (1996).

[8] C. J. Pethick and D. G. Ravenhall, Ann. Rev. Nucl. Part. Sci. **45**, 429 (1995).

[9] W. Nazarewicz, Nucl. Phys.**A 654**, 195c (1999).

[10] D.J. Morrissey and B. M. Sherrill, Phil. Trans. R. Soc. Lond A 356, 1985 (1998)

[11] H. Xu, M.B. Tsang et al., Phys. Rev. Lett. (in press)

[12] M.B. Tsang, W.A. Friedman, et al., to be published

[13] M. Weber et al., Z. Physik **A 343**, 67 (1992); Nucl.Phys. **A 578**, 659 (1994)

[14] R. Pfaff, Phd Thesis; R. Pfaff, D.J. Morrisey, W. Benenson, M. Fauerbach, M Hellstrom, C.F. Powell, B.M. Sherrill, M. Steiner, and J.A. Winger, Phys. Rev. **C 53**, 1753 (1996).

[15] K. Summerer and B. Blank, Phys. Rev. **C 60**, 034607 (2000).

[16] L.F. Oliveira, R. Donangelo, O. Rasmussen, Phys. Rev.**C 19**, 826 (1979).

[17] J.-J. Gaimard and K.-H. Schmidt Nucl. Phys. **A 531**, 709 (1991).

[18] J. Benlliure, K.-H.Schmidt, D. Cortina-Gil, T. Enqvist, F. Farget, A. Heinz, A.R. Junghans, J. Pereira, and J.Taieb, Nucl. Phys. **A 660**, 87 (1999).

[19] J. Gosset, H.H. Gutbrod, W.G. Meyer, A.M. Poskanzer, A. Sandival, R. Stock, and G.D. Westfall, Phys. Rev. **C 16**, 629 (1977).

[20] W.A. Friedman Phys. Rev.**C 27**, 569 (1983).

[21] W. Friedman and W. Lynch, Phys. Rev.**C 28**, 950 (1983).

[22] K.-H. Schmidt, private communications. Even though the code [18] used the excitation 27 MeV per abraded nucleon instead of 13.3 as indicated in the present work, the main differences are the yields of the neutron-deficient isotopes.

[23] Roman Gernhaeuser et al., Ph.D. Thesis, Techn. Univ. Muenchen, 1998 (unpublished).

Figure Captions:

Fig. 1: The relative isotope ratio, $R_{21}(N,Z) = Y_{^{86}Kr}(N,Z)/Y_{^{78}Kr}(N,Z)$ as a function of N for Z=23-36. Left hand panel: Data are represented by solid (even-Z) and open (odd-Z) points. The solid and dash lines are drawn to guide the eye. Right hand panel: The solid (even-Z) and dash (odd-Z) lines are ratios computed from EPAX2.

Fig. 2: Isotope distributions from the projectile fragmentation of ^{86}Kr [13] (top panels) and ^{78}Kr [14] (bottom panels). The distributions are offset by factors of 100 (See text for detailed explanations). Solid lines are predictions from the A-A model while the dashed lines are predictions from the EPAX2 calculations.

Fig. 3: Fragmentation of ^{86}Kr to produce Ni isotopes according to the Abrasion-Ablation model. ^{86}Kr was plotted at Z=36 and N=50. Open points represent the mean intermediate stages of the nuclei formed after the abrasion process. The dashed lines represent the avearge evaporation paths of the from the intermediate nuclei to the final Ni isotopes which are represented by the closed points along Z=28.

Fig. 4: Calculated cross-sections of ^{78}Ni from the fragmentation of Kr isotopes. The dot-dashed line extending from ^{86}Kr to ^{96}Kr. The open (truncated n-fluctuations) and solid (untruncated n-fluctuations) points are predictions from the A-A model. The solid curve at the bottom illustrate the relative production gains in a two step process of using the fragmentation of ^{100}Mo to produce the Kr isotopes first before ^{78}Ni is produced from the fragmentation of the Kr isotopes.

Fig. 5: Isotope distributions from the projectile fragmentation of ^{96}Zr [22] for Z=30-40. The distributions are offset by factors of 100 (See text for detailed explanations). Solid lines are predictions from the A-A model while the dashed lines are predictions from the EPAX2 calculations.

Fig1

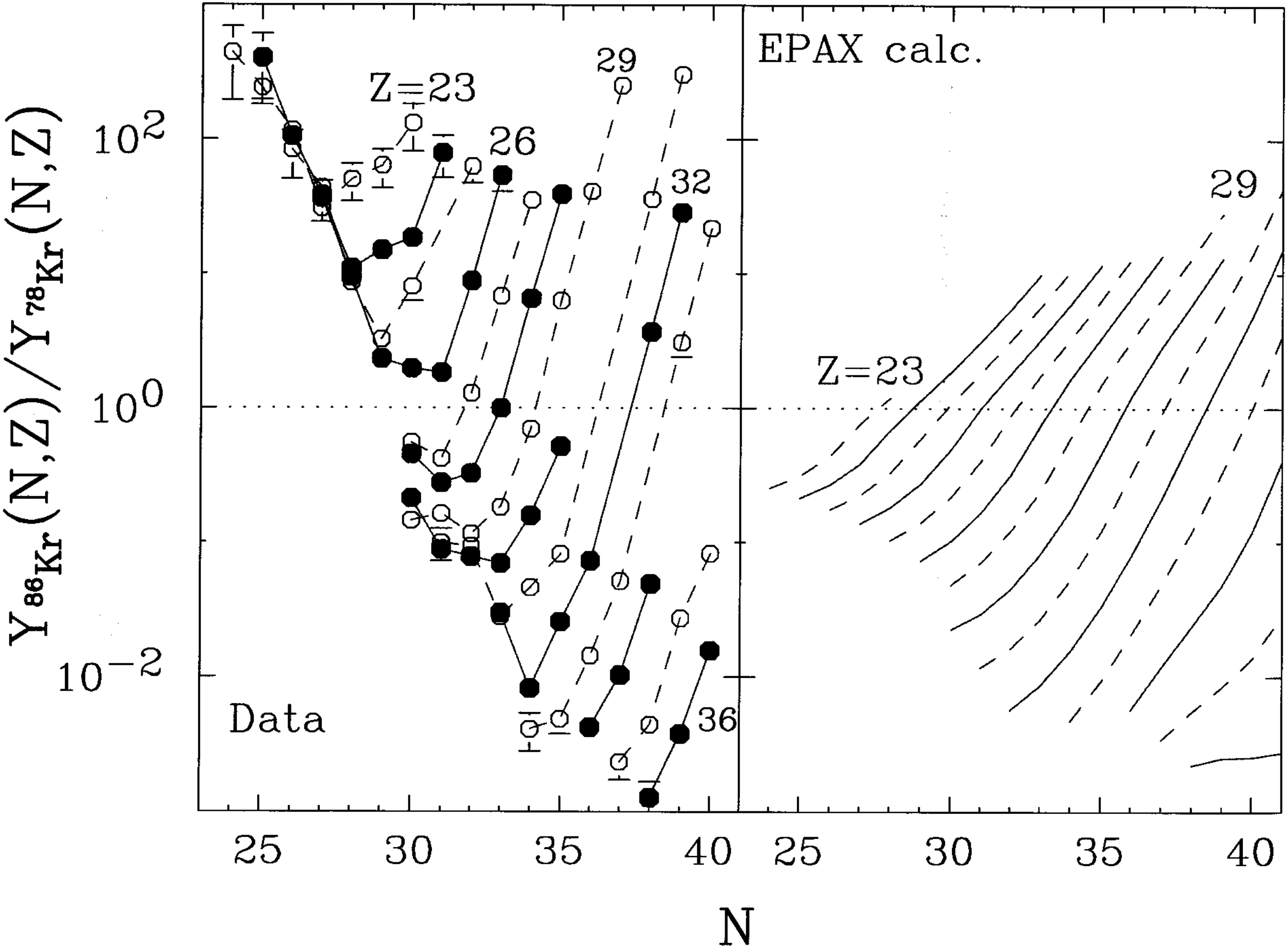

$Y_{^{86}Kr}(N,Z)/Y_{^{78}Kr}(N,Z)$
10^2
10^0
10^{-2}
Data
Z=23
26
29
32
36
EPAX calc.
Z=23
29
25
30
35
40
N

Fig 2

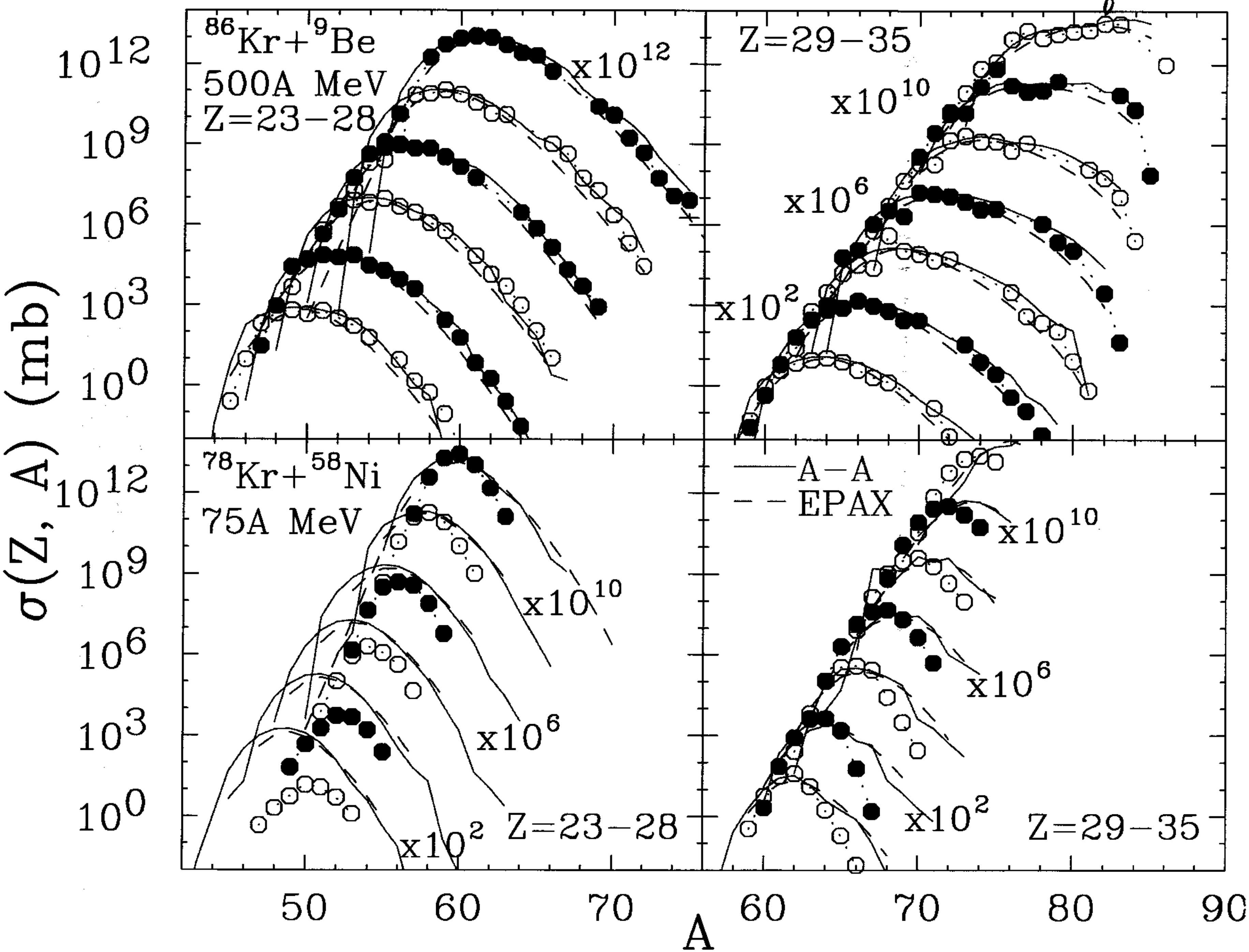

σ(Z, A) (mb)
A
86Kr+9Be
500A MeV
Z=23−28
Z=29−35
78Kr+58Ni
75A MeV
A−A
EPAX
x10^12
x10^10
x10^6
x10^2

Fig 3

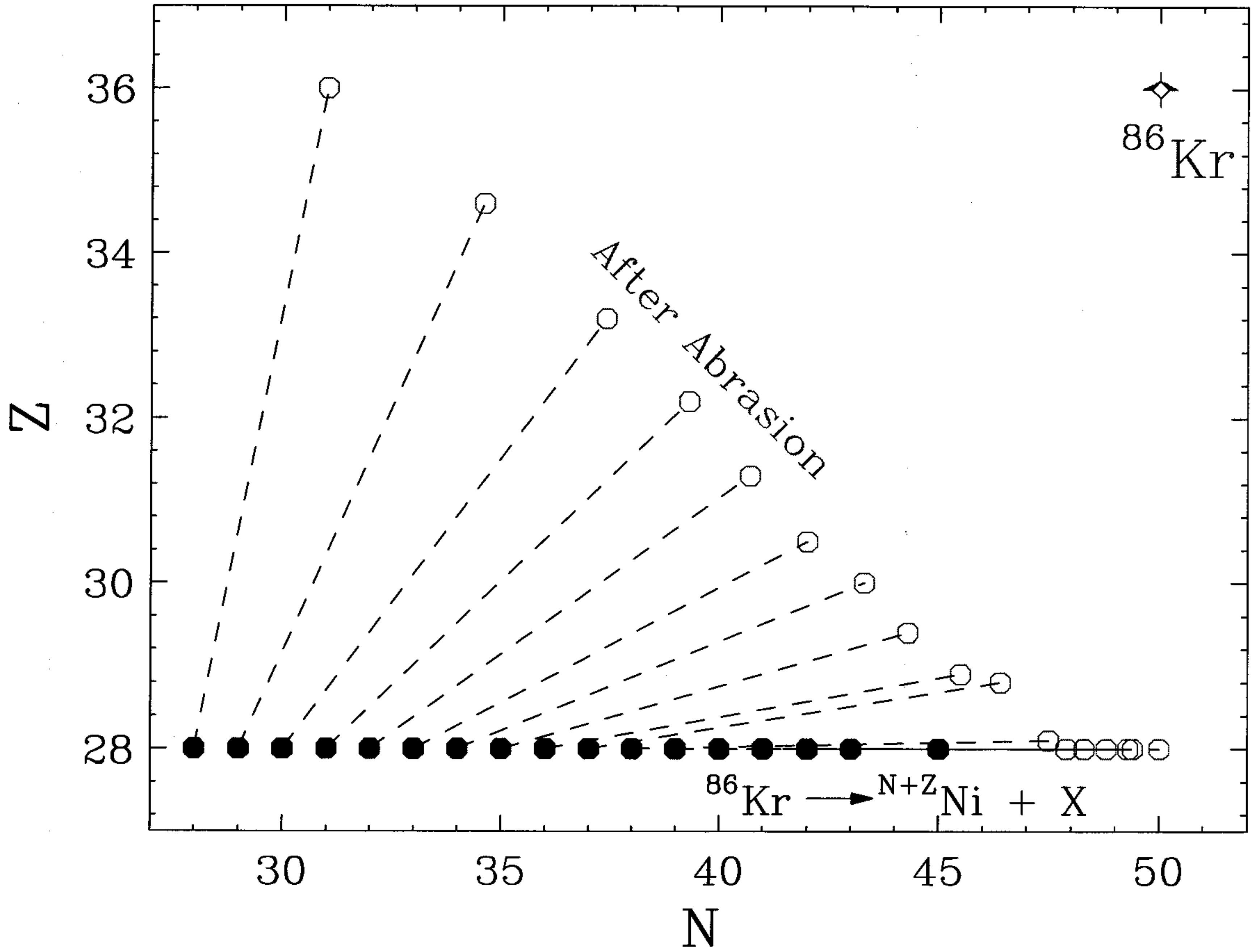

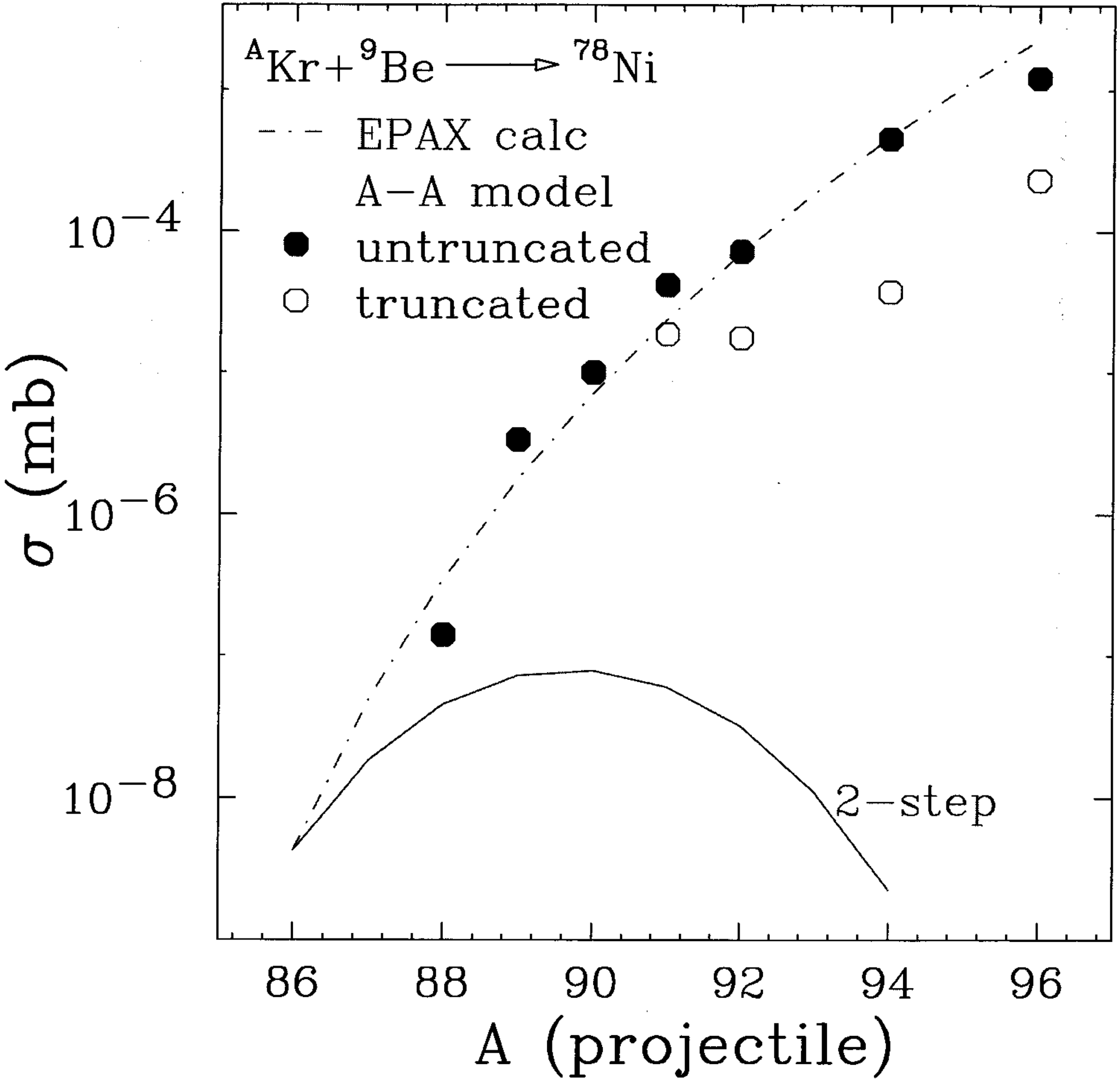

$^{A}Kr + ^{9}Be \longrightarrow ^{78}Ni$
EPAX calc
A–A model
untruncated
truncated
2–step
σ (mb)
10^{-4}
10^{-6}
10^{-8}
86
88
90
92
94
96
A (projectile)

Fig 4

Fig 5